

Raman scattering study of bulk and nanocrystalline PbMoO₄ at high pressures

R. Vilaplana, O. Gomis, F. J. Manjón, P. Rodríguez-Hernández, A. Muñoz et al.

Citation: *J. Appl. Phys.* **112**, 103510 (2012); doi: 10.1063/1.4765717

View online: <http://dx.doi.org/10.1063/1.4765717>

View Table of Contents: <http://jap.aip.org/resource/1/JAPIAU/v112/i10>

Published by the [American Institute of Physics](#).

Related Articles

Effect of Li⁺ ions on enhancement of near-infrared upconversion emission in Y₂O₃:Tm³⁺/Yb³⁺ nanocrystals
J. Appl. Phys. **112**, 094701 (2012)

Long range coupling between defect centres in inorganic nanostructures: Valence alternation pairs in nanoscale silica
J. Chem. Phys. **137**, 154313 (2012)

Pressure dependence of the Verwey transition in magnetite: An infrared spectroscopic point of view
J. Appl. Phys. **112**, 073524 (2012)

Silver nanoisland enhanced Raman interaction in graphene
Appl. Phys. Lett. **101**, 153113 (2012)

Chemical pressure effect on optical properties in multiferroic bulk BiFeO₃
J. Appl. Phys. **112**, 073516 (2012)

Additional information on J. Appl. Phys.

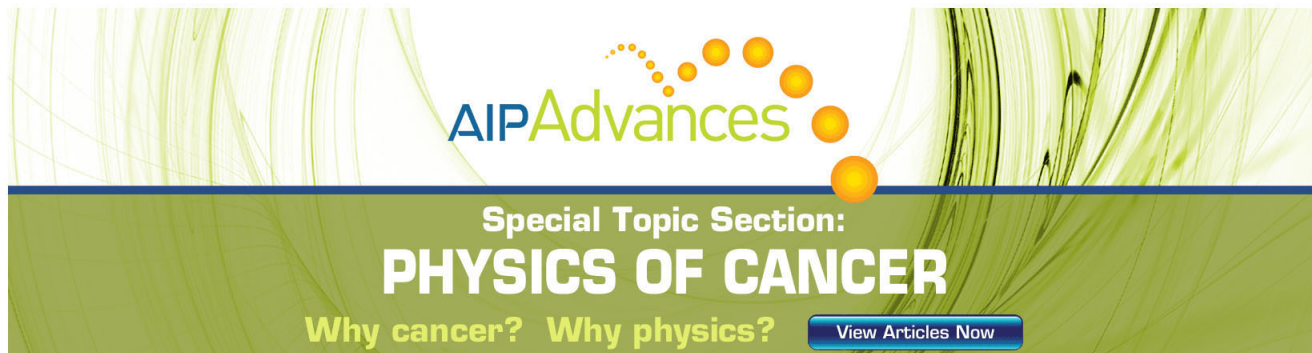
Journal Homepage: <http://jap.aip.org/>

Journal Information: http://jap.aip.org/about/about_the_journal

Top downloads: http://jap.aip.org/features/most_downloaded

Information for Authors: <http://jap.aip.org/authors>

ADVERTISEMENT



AIP Advances

Special Topic Section:
PHYSICS OF CANCER

Why cancer? Why physics? [View Articles Now](#)

Raman scattering study of bulk and nanocrystalline PbMoO₄ at high pressures

R. Vilaplana,¹ O. Gomis,¹ F. J. Manjón,^{2,a)} P. Rodríguez-Hernández,³ A. Muñoz,³ D. Errandonea,⁴ S. N. Achary,⁵ and A. K. Tyagi⁵

¹Centro de Tecnologías Físicas: Acústica, Materiales y Astrofísica, MALTA Consolider Team, Universitat Politècnica de València, 46022 València, Spain

²Instituto de Diseño para la Fabricación y Producción Automatizada, MALTA Consolider Team, Universitat Politècnica de Valencia, 46022 València, Spain

³Departamento de Física Fundamental II, Instituto de Materiales y Nanotecnología, MALTA Consolider Team, Universidad de La Laguna, 38205 Tenerife, Spain

⁴Departamento de Física Aplicada - ICMUV, MALTA Consolider Team, Universitat de València, Edificio de Investigación, c/ Dr. Moliner 50, 46100 Burjassot (València), Spain

⁵Chemistry Division, Bhabha Atomic Research Centre, Trombay, Mumbai 400085, India

(Received 30 April 2012; accepted 17 October 2012; published online 21 November 2012)

High-pressure Raman scattering measurements have been performed in wulfenite (PbMoO₄) for both bulk and nanocrystalline powders up to 22 GPa. Our Raman scattering measurements evidence the phase transition from the tetragonal scheelite structure to the monoclinic M-fergusonite structure in both bulk and nanocrystalline powders above 10.8 and 13.4 GPa, respectively. The pressure dependences of the Raman active modes in both structures were compared and discussed based on our theoretical results obtained from lattice dynamics *ab initio* calculations. © 2012 American Institute of Physics. [<http://dx.doi.org/10.1063/1.4765717>]

I. INTRODUCTION

Lead molybdate (PbMoO₄), also known by its mineral name wulfenite because of its discoverer the Austrian mineralogist F. X. von Wulffen (1728–1805), occurs as a secondary mineral in the hydrothermal oxidation zone of lead deposits at the earth mantle. At ambient conditions, PbMoO₄ crystallizes in the tetragonal scheelite-type structure [space group (S.G.) I4₁/a, No. 88, Z = 4].¹ In this structure each Pb atom is coordinated to eight O atoms, and each Mo atom is coordinated to four O atoms. Wulfenite has attracted considerable attention due to its acousto-optical, photoconductivity, luminescence, photocatalyst, and thermoluminescence properties.^{2–5} In particular, PbMoO₄ is a potential material for cryogenic detectors of double-beta decay experiments.⁴ The diversified properties of PbMoO₄, even though attracted intense research for quite a long time, are still not known because there is a lack of fundamental understanding of its thermodynamic properties.⁴

Pressure is an important thermodynamic parameter, and high-pressure studies are extremely important to understand the physical, chemical, and mechanical properties of materials. High-pressure research has proven to be an efficient tool to improve the understanding of the main physical-chemical properties of scheelite-structured oxides.⁶ In particular, scheelite-type PbWO₄, whose mineral name is stolzite, has been found to undergo phase transitions to the monoclinic M-fergusonite structure (S.G. I2/a), hereafter named only as fergusonite, and to the monoclinic BaWO₄-II structure (S.G. P2₁/n).^{7,8} These phase transitions are common to AWO₄ compounds with A = Ca, Sr, and Ba.^{8–10} Since AWO₄

and AMoO₄ compounds are very similar from crystal chemical considerations,⁶ we expect that PbMoO₄ undergoes pressure-induced phase transitions similar to those of PbWO₄ and related to those that have been already found in CaMoO₄, SrMoO₄, CdMoO₄, EuMoO₄, and BaMoO₄.^{11–17}

Wulfenite was studied at high pressures by Raman scattering up to 3.5 GPa in the late 1970s by Ganguly and Nicol using NaCl as pressure-transmitting medium, and no phase transition was observed.¹⁸ Later, Hazen *et al.* performed x-ray diffraction (XRD) measurements up to 6 GPa, and no phase transition was reported.¹⁹ Jayaraman *et al.* performed Raman scattering measurements till 11 GPa, with a 4:1 methanol-ethanol mixture as a pressure-transmitting medium and found a phase transition to an unknown structure at 9.5 GPa.²⁰ However, more recent Raman scattering measurements up to 26.5 GPa performed by Yu *et al.* under non-hydrostatic conditions²¹ evidenced a different phase transitions sequence, viz., which ended in a transition to an amorphous phase around 12.5 GPa. This observation was in total disagreement with the results previously published on PbMoO₄. In 2009, Liu *et al.* reported x-ray diffraction measurements up to 23 GPa and showed that PbMoO₄ undergoes a phase transition to the M-fergusonite structure around 10.6 GPa.²² Recently, a similar result was found by Errandonea *et al.* who also studied for the first time the behavior of PbMoO₄ nanocrystals at high pressures.²³ These authors found that while bulk wulfenite undergoes a phase transition to the M-fergusonite phase around 10.7 GPa, the phase transition was not observed even up to 16 GPa in nanocrystals.

In this work we report Raman scattering measurements up to 22 GPa in bulk and nanocrystalline PbMoO₄. Our measurements support the reversible second-order phase transition to the M-fergusonite structure in both bulk and nanocrystalline wulfenite above 10.8 and 13.4 GPa, respectively. Furthermore,

^{a)}Author to whom correspondence should be addressed. Electronic mail: fjmanjon@fis.upv.es.

our experimental results are compared to previous studies in other molybdates and to *ab initio* lattice dynamics calculations that have allowed us to interpret and assign the Raman-active modes in the scheelite and fergusonite structures.

II. EXPERIMENTAL DETAILS

Details of the preparation procedure of both bulk and nanocrystalline powder samples of PbMoO₄ from its constituents are given in Ref. 23. XRD measurements were performed in order to check the tetragonal scheelite structure of wulfenite in both bulk and nanocrystalline samples. No other spurious phases were detected. The average particle size in nanocrystalline samples, as estimated by Scherrer formula, was around 20–25 nm. For high-pressure measurements, the samples were loaded with a 4:1 methanol-ethanol mixture as a pressure-transmitting medium in the 150 μm diameter hole of an Inconel gasket inside a membrane-type diamond anvil cell (DAC). High-pressure Raman scattering measurements at room temperature were performed with a LabRAM HR UV micro spectrometer coupled to a Peltier-cooled CCD camera and using a 632.81 nm (1.96 eV) HeNe laser excitation line with a power of 10 mW and a spectral resolution better than 2 cm⁻¹. In order to analyze the Raman spectra under pressure, Raman peaks have been fitted, when possible, to a Voigt profile (Lorentzian profile convoluted by a Gaussian due to the limited resolution of the spectrometer) where the spectrometer resolution is a fixed parameter. Pressure was determined by the ruby luminescence method.²⁴

III. AB INITIO CALCULATIONS

In order to further strengthen the conclusions obtained from our Raman study, *ab initio* calculations of the bulk phonon modes for the scheelite and fergusonite phases at the Brillouin zone (BZ) center (Γ point) were performed. All the calculations were done within the framework of the density functional theory (DFT) using the Vienna *ab initio* simulation package (VASP).²⁵ The exchange and correlation energy were taken in the generalized gradient approximation (GGA) according to Perdew-Burke-Ernzerhof (GGA-PBE). The projector-augmented wave (PAW) scheme²⁶ was adopted, and the semicore 5d electrons of Pb were dealt explicitly in the calculations. The set of plane waves used were extended up to a kinetic energy cutoff of 520 eV. This large cutoff was required to deal with the O atoms within the PAW scheme to ensure highly converged results. A dense k-points grid is used for integrations along the BZ, which ensure us highly converged results to about 1 meV per formula unit. At each selected volume, the structures were fully relaxed to their equilibrium configuration through the calculation of the forces on atoms and the stress tensor. In the relaxed equilibrium configuration, the forces are smaller than 0.004 eV/Å, and the deviation of the stress tensor from a diagonal hydrostatic form is smaller than 1 kbar. Our calculations are performed for the different structures that we consider in the following way. We calculate for different volumes the total energy, E (at T = 0 K), from the *ab initio* program, relaxing the structure, and from the stress tensor we can obtain directly the theoretical pressure, P, for a

selected volume, V, providing also the external and internal structural parameters at the selected volume. This allows us to have an E(V,P) set of data that can be fitted with an equation of state (EOS). Having the E, V, and P data for different structures at T = 0 K, a phase transition between two different structures 1 and 2 will occur when the enthalpy is the same for a certain pressure P_t, E₁ + P_t·V₁ = E₂ + P_t·V₂, where P_t is the theoretical transition pressure.

The application of DFT-based total-energy calculations to the study of semiconductor's properties under high pressure has been reviewed in Ref. 27, where it has been shown that the phase stability, electronic, and dynamical properties of compounds under pressure are well described by DFT. For the study of the dynamical properties, we perform the calculations by the direct method in order to obtain the dynamical matrix and the phonons at the Γ point, as described in Ref. 9. In this study we only present DFT studies for PbMoO₄ bulk material. The study of nanocrystalline phases using DFT methods requires a unit cell with hundreds of atoms and many degrees of freedom; therefore, this kind of system is out of the actual capabilities of our computational method.

IV. RESULTS AND DISCUSSION

A. Scheelite structure

As mentioned earlier, PbMoO₄ crystallizes at ambient conditions in the centrosymmetric scheelite structure [SG I4₁/a (C_{4h}⁶)], where Pb and Mo atoms occupy S₄ sites whereas O atoms are on general C₁ sites. Group theoretical considerations lead us to expect 13 Raman-active modes at the Γ point.⁷

$$\Gamma = \nu_1(A_g) + \nu_2(A_g) + \nu_2(B_g) + \nu_3(B_g) + \nu_3(E_g) + \nu_4(B_g) + \nu_4(E_g) + R(A_g) + R(E_g) + 2T(B_g) + 2T(E_g). \quad (1)$$

The modes with A_g and B_g symmetry are single modes while those with E_g symmetry are doubly degenerated. Translational (T) modes and rotational (R) modes are considered to be the external modes of the MoO₄ tetrahedra and are the smallest in frequency. The rest of the modes (ν₁ to ν₄) are considered to be the internal modes (stretching and bending) of the MoO₄ tetrahedra and are higher in frequency, being the stretching modes the highest in frequency. In the following we will also denote the different A_g, B_g, and E_g modes by a superscript which numbers the modes in terms of increasing frequency. In particular we use this notation to distinguish between the two translational E_g and B_g modes of the scheelite structure and to number the A_g and B_g modes of the fergusonite structure in Sec. IV B.

Figure 1 shows Raman spectra of bulk PbMoO₄ up to 10 GPa separated into two frequency regions. Raman spectra should correspond to a mixture of polarizations perpendicular and parallel to the c-axis because of the arbitrary orientation of powders inside the DAC. The Raman spectrum of bulk wulfenite at 1 atm is dominated by the stretching ν₁(A_g³) mode near 906 cm⁻¹. Other eleven modes have been

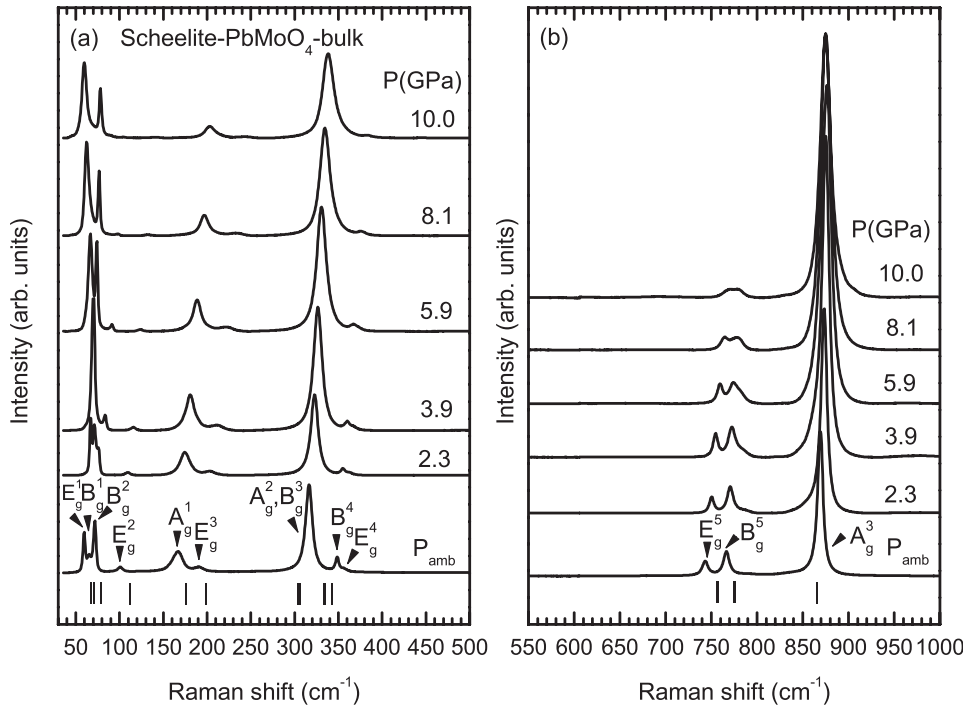


FIG. 1. Room-temperature Raman spectra of bulk scheelite-PbMoO₄ at different pressures between 1 atm and 10 GPa: (a) low-frequency region and (b) high-frequency region. Bottom marks indicate the *ab initio* calculated frequencies of the Raman-active modes of the scheelite phase at 1 atm.

identified, so we have followed the pressure dependence of a total of twelve Raman modes; i.e., the same number of Raman modes as Jayaraman *et al.*²⁰ and one mode more than Ganguly and Nicol.¹⁸ The only mode which has not been measured is either the $\nu_2(A_g^2)$ or $\nu_2(B_g^3)$ near 320 cm^{-1} . According to our calculations these modes are so close to each other that one of them is masked by the other one. Note that both Ganguly *et al.* and Jayaraman *et al.* also reported a single mode in this frequency region.^{18,20} However, unlike previous measurements,^{18,20} we have been able to resolve the $\nu_4(B_g^4)$ and $\nu_4(E_g^4)$ modes near 350 cm^{-1} . Curiously, Jayaraman *et al.* did also measure two Raman modes in this

frequency region at some pressures. However, these authors did not report the pressure coefficient of the high-frequency mode, which we have attributed to the $\nu_4(E_g^4)$ mode on the basis of our theoretical calculations.

Figure 2 shows the pressure dependence of the experimental (symbols) and theoretical (lines) Raman mode frequencies of bulk PbMoO₄ up to 20 GPa. In the region 0–10 GPa (left panel of Fig. 2), it can be observed that all modes corresponding to the scheelite phase exhibit a positive pressure coefficient except one mode that shows a negative pressure coefficient (soft mode). Table I summarizes the experimental and theoretical frequencies and pressure

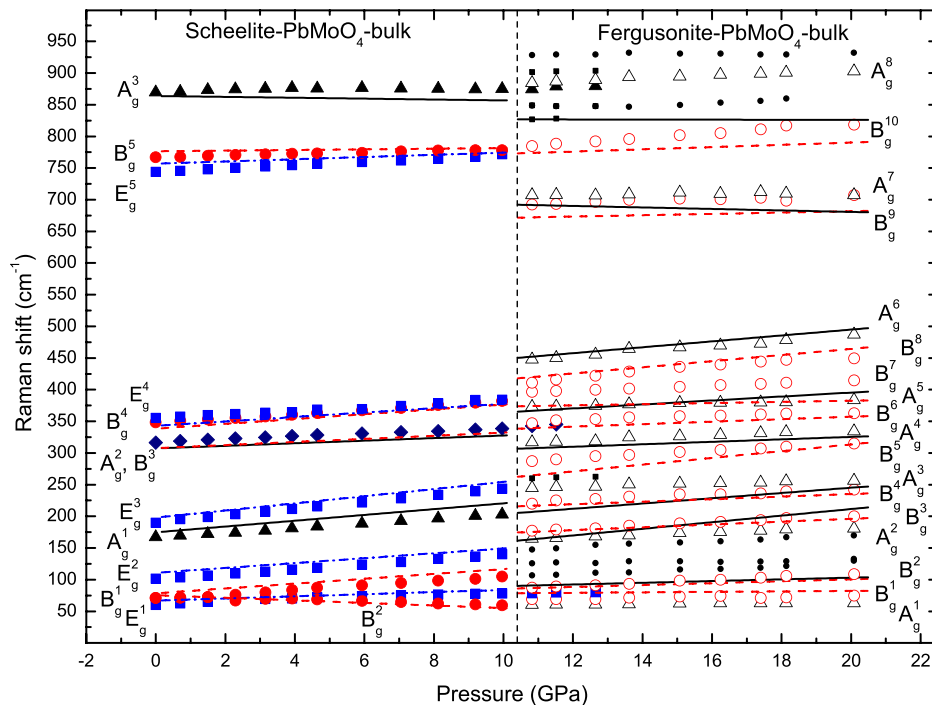


FIG. 2. Experimental (symbols) and theoretical (lines) pressure dependence of the frequencies of the first-order Raman modes of the scheelite (left) and fergusonite (right) phases for bulk PbMoO₄ up to 20 GPa. Solid (open) black triangles, red circles, and blue squares represent the experimental A, B, and E modes of the scheelite (fergusonite) phase whereas black solid, red dashed, and blue dotted-dashed lines represent theoretical A, B, and E modes. Solid diamonds represent a single peak assigned to a mixture of two different Raman modes. In the right panel small circles (squares) refer to IR-active or second-order modes of the fergusonite (scheelite) phase.

TABLE I. *Ab initio* calculated (Th.) and experimental frequencies and pressure coefficients of the Raman modes in scheelite-type PbMoO₄ at 1 atm. Experimental data of bulk and nanocrystalline (Nano.) material are reported.

Peak/mode	Th.		Bulk		Nano.	
	ω (0) (cm ⁻¹)	d ω /dP (cm ⁻¹ /GPa)	ω (0) (cm ⁻¹)	d ω /dP (cm ⁻¹ /GPa)	ω (0) (cm ⁻¹)	d ω /dP (cm ⁻¹ /GPa)
T (E _g ¹)	70.0 (5)	1.8 (1)	64 (1)	1.5 (2)	63.3 (8)	1.7 (1)
T (B _g ¹)	77 (1)	3.8 (2)	68.2 (8)	3.8 (1)	69 (1)	3.6 (1)
T (B _g ²)	71 (1)	-2.0 (2)	74.4 (8)	-1.1 (1)	73.1 (8)	-1.2 (1)
T (E _g ²)	110.7 (5)	3.85 (7)	99 (1)	4.6 (1)	101 (2)	3.9 (3)
R (A _g ¹)	174.7 (3)	4.58 (4)	164 (2)	4.5 (1)	167 (3)	3.7 (3)
R (E _g ³)	198.0 (2)	5.64 (2)	188 (2)	6.0 (1)	191 (2)	5.3 (2)
ν_2 (A _g ²)	307.2 (2)	2.03 (3)	318 (1)	2.1 (1)	318 (2)	2.1 (1)
ν_2 (B _g ³)	307.6 (3)	2.44 (4)	318 (1)	2.1 (1)	318 (2)	2.1 (1)
ν_4 (B _g ⁴)	338.4 (5)	3.81 (6)	348 (2)	3.4 (1)	347 (3)	3.9 (1)
ν_4 (E _g ⁴)	343.0 (4)	3.46 (6)	355 (2)	2.9 (1)	356 (3)	3.0 (1)
ν_3 (E _g ⁵)	756.9 (6)	1.74 (9)	743 (1)	2.8 (1)	744 (2)	2.7 (1)
ν_3 (B _g ⁵)	776.4 (6)	0.51 (8)	770 (1)	0.9 (1)	768 (2)	1.2 (1)
ν_1 (A _g ³)	864 (1)	-0.7 (1)	873 (1)	0.2 (1)	872 (2)	0.4 (1)

coefficients as well as the symmetry of all the Raman modes in the scheelite phase of bulk PbMoO₄. As observed in Table I, our assignment of mode symmetries is in good agreement with that of Ganguly and Nicol.¹⁸ In this respect, our theoretical calculations confirm that the soft mode is the T(B_g²) mode. This is in agreement with the fact that the soft mode in all tungsten and molybdenum scheelites is one of the low-frequency B_g modes, which is related to a translation of the BO₄ tetrahedra ($B = W, Mo$) along the c -axis of the tetragonal structure.²⁸ As regards the measured pressure coefficients of the different Raman modes in scheelite-PbMoO₄, one can see that they also agree with our theoretical calculations and with those reported by Ganguly and Nicol¹⁸ and Jayaraman *et al.*²⁰

Figure 3 shows selected Raman spectra of nanocrystalline PbMoO₄ up to 12 GPa divided into two frequency

regions. Again, Raman spectra of nanocrystalline PbMoO₄ should correspond to a mixture of polarizations perpendicular and parallel to the c -axis because of the arbitrary orientation of powders inside the DAC. It can be observed that the Raman spectrum of nanocrystalline PbMoO₄, which is also dominated by the ν_1 (A_g³) mode, displays similar modes to those of the bulk material. In general, all Raman modes of the nanocrystalline powders are broader than those of the bulk material, so some Raman-active modes that are very close in frequency, like the ν_2 (A_g²) or ν_2 (B_g³) (near 320 cm⁻¹), have not been clearly resolved. In this respect, we have followed the pressure dependence of twelve modes in nanocrystalline PbMoO₄. Additionally, a broad band is observed in nanocrystalline powders between 600 and 700 cm⁻¹ [see asterisk in Fig. 3(b)], whose intensity decreases with increasing pressure and that it is not

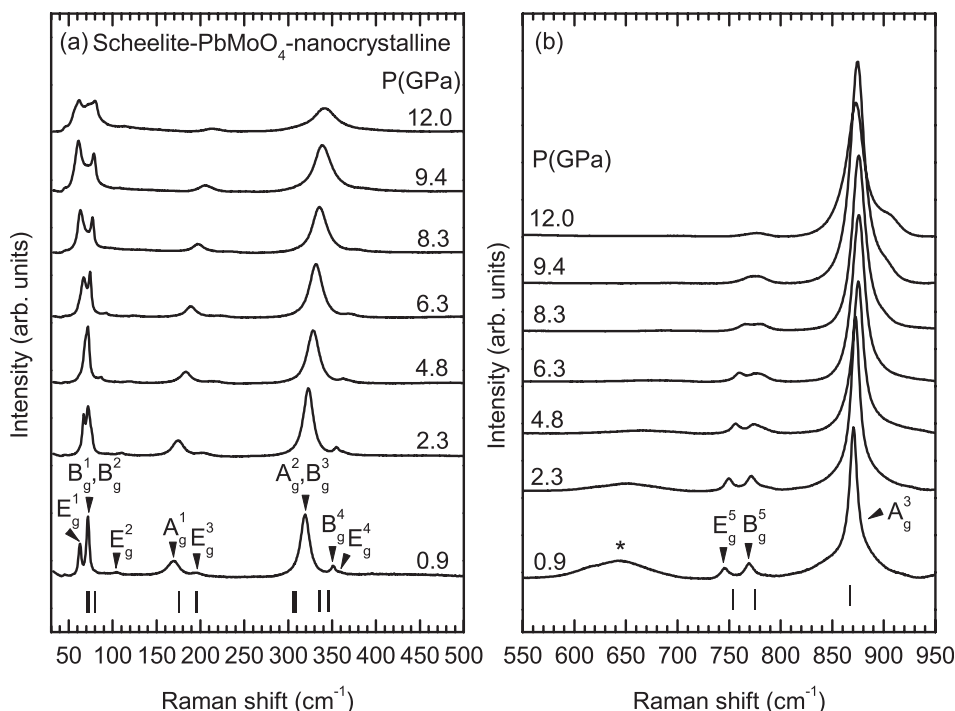


FIG. 3. Room-temperature Raman spectra of nanocrystalline scheelite-PbMoO₄ at different pressures between 1 atm and 12 GPa: (a) low-frequency region and (b) high-frequency region. Bottom marks indicate the *ab initio* calculated frequencies of the Raman-active modes of the scheelite phase at 1 atm.

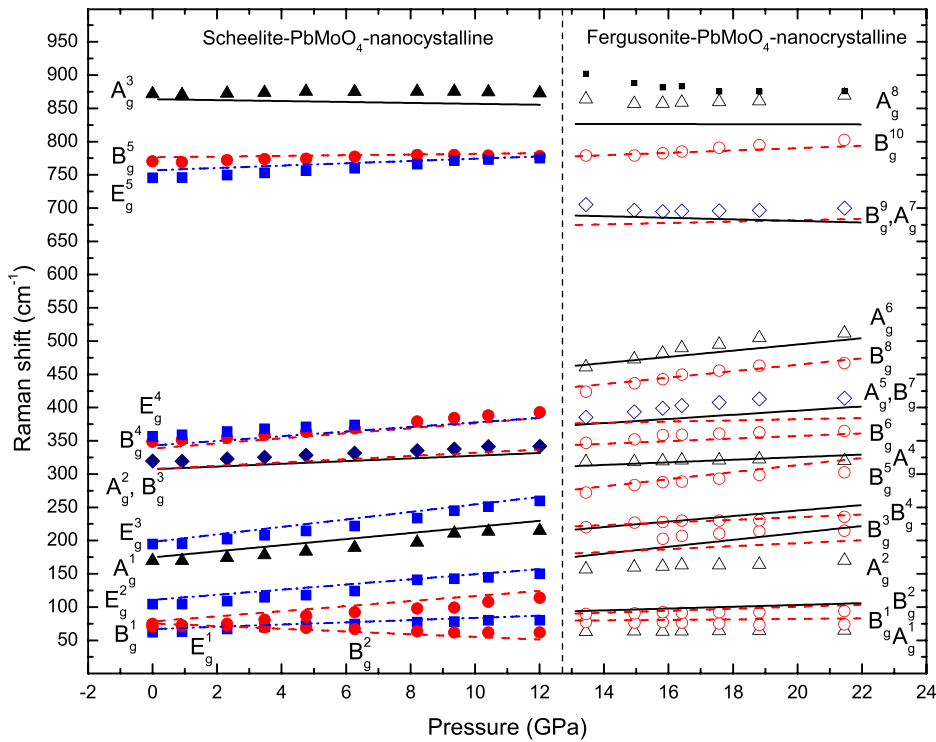


FIG. 4. Experimental (symbols) and theoretical (lines) pressure dependence of the Raman mode frequencies of the first-order modes of the scheelite (left) and fergusonite (right) phase of nanocrystalline PbMoO_4 up to 22 GPa. Solid (open) black triangles, red circles, and blue squares represent the experimental A , B , and E modes of the scheelite (fergusonite) phase whereas black solid, red dashed, and blue dotted-dashed lines represent theoretical A , B , and E modes as in Fig. 2. Solid diamonds represent a single peak assigned to a mixture of two different Raman modes. In the right panel second-order modes of the fergusonite phase are plotted with small solid squares.

observed in some regions of the sample. At present we have no definite explanation for the origin of this band, but it could correspond to a second-order Raman mode of the scheelite phase.

Figure 4 shows the pressure dependence of the experimental (symbols) and theoretical (lines) Raman mode frequencies of nanocrystalline PbMoO_4 up to 22 GPa. Table I summarizes the experimental frequencies and pressure coefficients of all the Raman modes in the scheelite phase of nanocrystalline PbMoO_4 , which can be compared to the experimental and theoretical mode frequencies and pressure coefficients of bulk PbMoO_4 . As observed in Table I, the frequencies and pressure coefficients of the Raman modes in nanocrystalline wulfenite are very similar to those of bulk wulfenite and agree with those theoretically calculated for bulk wulfenite.

Figure 5 shows with solid symbols the pressure dependence of the experimental full width at half maximum (FWHM) of some of the Raman-active modes in nanocrystalline PbMoO_4 up to 12 GPa. In Fig. 5 it is also shown with empty symbols the FWHM of the same Raman-active modes in bulk PbMoO_4 at 1 atm for comparison with the results of nanocrystalline PbMoO_4 . It is found that at 1 atm the FWHMs of Raman modes in nanocrystalline PbMoO_4 are slightly larger than the corresponding modes in the bulk material. The broadening of the modes in nanocrystalline wulfenite is rather symmetrical, thus suggesting that it is caused by the decrease of the grain size with respect to the bulk and by an homogeneous distribution in grain sizes around 20–25 nm. No mode-confinement effect leading to asymmetrical broadening of the Raman peaks is observed. This observation is in good agreement with previous reports suggesting that confinement is expected for grain sizes well below 10 nm.²⁹ On the other hand, the FWHM of all Raman modes of the scheelite phase increases as pressure increases. Note

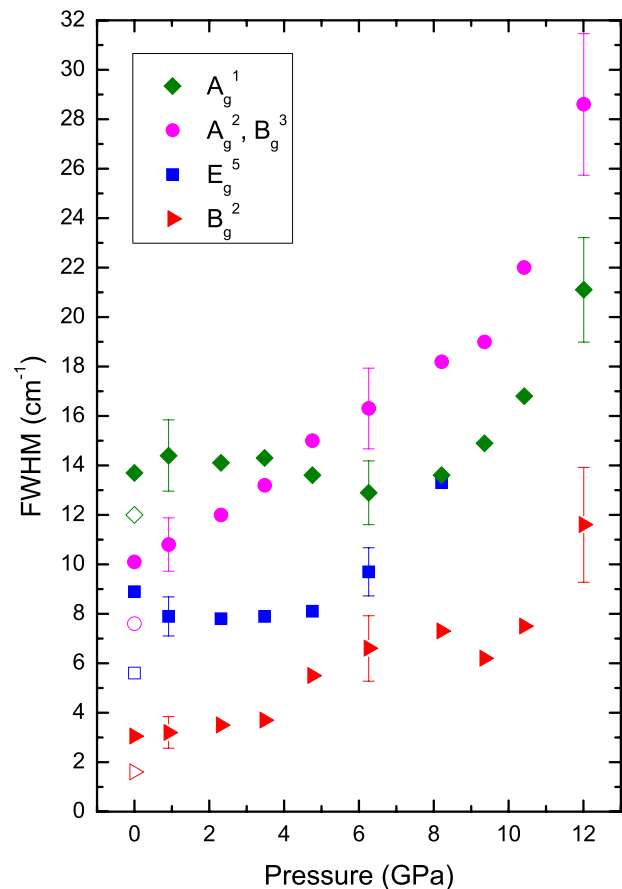


FIG. 5. Experimental pressure dependence of the FWHM of some Raman modes for the scheelite phase of nanocrystalline PbMoO_4 . The FWHM for the case of bulk PbMoO_4 is also included at 1 atm for comparison with the results for nanocrystals.

that there is not a uniform increase of the FWHM of all modes with increasing pressure. This means that the FWHM increase of each mode is related to the pressure dependence of the phonon-phonon decay processes particular for each phonon mode.^{30,31}

B. Fergusonite structure

New Raman modes appear in the Raman spectra of bulk and nanocrystalline PbMoO_4 above 10.8 and 13.4 GPa, respectively, thus suggesting a structural phase transition. According to recent XRD measurements at ambient pressure, there is a reversible second-order phase transition from the scheelite to the fergusonite structure around 10 GPa in bulk wulfenite.^{22,23} We will show in the following that our Raman measurements of the high-pressure phase are consistent with the fergusonite structure and with the reversibility and second-order nature of the scheelite-to-fergusonite phase transition. Furthermore, we will try to assign the symmetry of the Raman-active modes of the fergusonite phase with the help of lattice dynamics *ab initio* calculations.

Figure 6 shows Raman spectra of bulk PbMoO_4 from 10.8 GPa to 20 GPa divided into two frequency regions. The Raman spectrum at 10.8 GPa shows the presence of new Raman modes along with some coexisting Raman modes of the scheelite phase (marked with asterisks). Some of the strongest modes of the scheelite phase; i.e., the $T(E_g^1)$, $\nu_2(A_g^2)-\nu_2(B_g^3)$, and $\nu_1(A_g^3)$ modes persist in the Raman spectra recorded up to 12.6 GPa (see big solid symbols in Fig. 2). However, at 13.6 GPa many Raman modes become thinner due to the disappearance of the Raman modes of the scheelite phase that were overlapping with some modes of the high-pressure phase. Therefore, we can conclude that the phase transition in bulk PbMoO_4 is completed at 13.6 GPa.

In this way, the coexistence of both scheelite and high-pressure phases is evidenced only in about a 2 GPa pressure range. Figure 6 also shows the Raman spectrum taken at 1 atm after releasing pressure of bulk PbMoO_4 . This spectrum can be attributed to the scheelite phase; thus, it confirms the reversibility of the scheelite to fergusonite phase transition in bulk material.

The centrosymmetric monoclinic fergusonite structure ($I2/a$, SG No. 15, $Z=4$) should have 36 vibrational modes at the zone centre, with the following mechanical representation:⁷

$$\Gamma = 8A_g + 8A_u + 10B_g + 10B_u. \quad (2)$$

The 18 gerade (g) modes are Raman active and the 18 ungerade (u) modes are IR active. The 18 Raman-active modes derive from the reduction of the tetragonal C_{4h} symmetry of the scheelite structure to the monoclinic C_{2h} symmetry of the fergusonite structure. In particular, every A_g and every B_g mode of the scheelite phase transforms into an A_g mode of the fergusonite phase, while every doubly degenerate E_g mode from the scheelite phase transforms into two B_g modes of the monoclinic symmetry.

Figure 6 shows the assignment of Raman modes to the fergusonite phase (see black arrows) at 13.6 GPa according to the *ab initio* calculations at a similar pressure. It can be observed that more Raman modes appear in the Raman spectrum than those predicted for the fergusonite phase (see red arrows and exclamation marks). However, it is noteworthy that the Raman spectra of the high-pressure phase of bulk PbMoO_4 are characterized by a gap between 500 and 650 cm^{-1} without first-order Raman bands. This feature has been already observed in the fergusonite phase of tungstates^{7,9} and, together with the similar phase transition

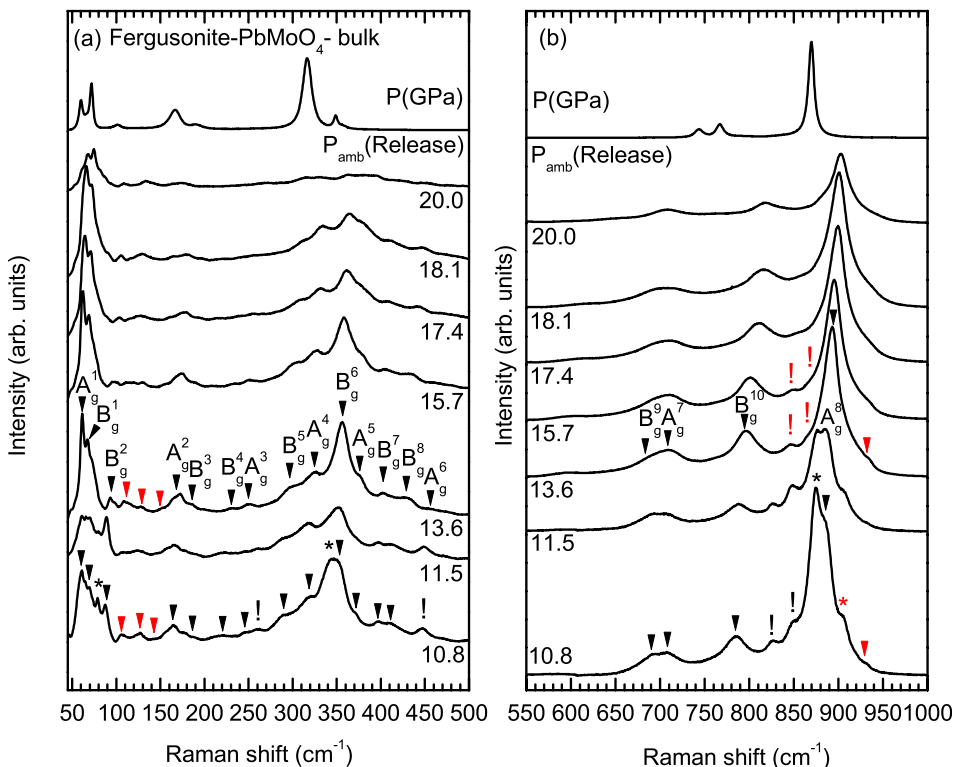


FIG. 6. Room-temperature Raman spectra of the fergusonite phase of bulk PbMoO_4 at different pressures between 10.8 and 20.0 GPa: (a) low-frequency region and (b) high-frequency region. Black (red) arrows indicate the first-order (second-order) Raman modes of the fergusonite phase. Black (red) asterisks correspond to first-order (second-order) Raman modes of the remaining scheelite phase. Black (red) exclamation marks correspond to modes assigned to IR-active modes of the scheelite (fergusonite) phase. The assignment of the first-order Raman-active modes in the fergusonite phase is shown in the Raman spectrum at 13.6 GPa. The Raman spectrum at 1 atm after releasing pressure is also shown.

pressure found in previous XRD measurements,^{22,23} support our assignment of the high-pressure phase of bulk wulfenite to the fergusonite structure.

Due to the group-subgroup relationship between the scheelite and fergusonite structures, the three high-frequency modes [$\nu_3(\text{B}_g^5)$, $\nu_3(\text{E}_g^5)$, and $\nu_1(\text{A}_g^3)$] of the scheelite phase in PbMoO_4 , corresponding to the stretching modes of the MoO_4 molecule, should transform into four modes [B_g^9 , A_g^7 , B_g^{10} , and A_g^8] of the fergusonite structure; however, more than four Raman modes are observed in the high-frequency region of the Raman spectra of bulk PbMoO_4 [see Fig. 6(b)]. A similar observation in previous high-pressure Raman scattering measurements of BaMoO_4 (Refs. 14 and 15) forced Christofilos *et al.* to conclude that the high-pressure phase of BaMoO_4 was not likely the fergusonite structure.¹⁴ However, the fergusonite structure of high-pressure phase of BaMoO_4 and PbMoO_4 has been confirmed by the most recent XRD measurements.^{15,22,23}

The above discrepancies between the Raman and XRD measurements of the high-pressure phase of BaMoO_4 and PbMoO_4 can be solved if we make some additional considerations regarding the Raman spectrum of the possible high-pressure phases. In particular, if the stretching mode of higher intensity in the scheelite phase, the $\nu_1(\text{A}_g^3)$ mode, transforms into the A_g^8 mode of the fergusonite structure, one would expect to have only one mode of high intensity in the fergusonite phase. This is indeed what we have observed in bulk PbMoO_4 above 13.6 GPa and what was previously observed in BaMoO_4 between 5.8 and 9.0 GPa.^{14,15} Therefore, the Raman modes observed above 13.6 GPa are consistent with the fergusonite nature of the high-pressure phase in these molybdates. A different case occurs for the high-pressure phase of PbWO_4 where two strong peaks appear in the Raman spectra of the high-pressure phase above 6.2 GPa near the $\nu_1(\text{A}_g^3)$ mode of the scheelite phase. Those two peaks were assigned to the monoclinic PbWO_4 -III phase, which has more Raman-active modes than the fergusonite phase.⁷ Therefore, we are confident that the high-pressure phase of bulk wulfenite is the monoclinic fergusonite phase.

As regards the nature of the additional peaks that appear in the Raman spectra above 10.8 GPa, which do not correspond to first-order modes of the fergusonite phase, we want to note that weak Raman bands were previously observed both at $820\text{--}824\text{ cm}^{-1}$ and at $851\text{--}859\text{ cm}^{-1}$ and assigned to the strain-activated infrared $\nu_3(\text{A}_u)$ and $\nu_1(\text{B}_u)$ modes of the scheelite phase of wulfenite at ambient pressure.^{32,33} Therefore, we think that the two bands observed above 10.8 GPa at lower frequencies than the $\nu_1(\text{A}_g^3)$ and A_g^8 modes of the scheelite and fergusonite phases, respectively, could be tentatively attributed to the strain-activated $\nu_3(\text{A}_u)$ and $\nu_1(\text{B}_u)$ infrared modes of the scheelite phase [see black exclamation marks in Fig. 6(b)]; however, it cannot be discarded that they could be second-order modes of the scheelite phase. Note that non-hydrostatic components of strain inside the samples can be induced at pressures near the scheelite-to-fergusonite phase transition despite such non-hydrostatic components are not evidenced by the ruby luminescence in the pressure-transmitting medium. It is also noteworthy that above 13.6 GPa the mode near 825 cm^{-1} disappears while the

mode near 850 cm^{-1} decreases in intensity and shifts a little bit in frequency. Additionally, a new mode appears as a weak shoulder (860 cm^{-1}) of the A_g^8 mode of the fergusonite phase. We have tentatively attributed these two latter modes [see red exclamation marks in Fig. 6(b)] above 13.6 GPa to the strain-activated B_u^{10} and A_u^8 IR modes with highest frequency in the fergusonite phase, but again we cannot discard that they could be second-order modes of the fergusonite phase. Note that the weak shoulder around 860 cm^{-1} was barely observed in the Raman spectra at 13.6 and 15.7 GPa but not at higher pressures; consequently its pressure dependence has not been plotted in right panel of Fig. 2.

On the other hand, we have to note that there are other modes above 10.8 GPa that do not correspond to first-order modes of the fergusonite phase. The two bands that appear at higher frequencies than the $\nu_1(\text{A}_g)$ and A_g^8 modes of the scheelite and fergusonite phases [see red asterisk and arrow in Fig. 6(b)] are likely due to second-order Raman modes of the scheelite and fergusonite phases because the one at lower frequency is no longer present in the spectrum at 13.6 GPa while the second one is observed till the highest pressure reached in the experiment. Finally, there are strong modes at 260 and 445 cm^{-1} [see black exclamation marks in Fig. 6(a)] that appear as strong modes in the Raman spectra between 10.8 and 12.6 GPa. They do not correspond neither to the fergusonite phase since they are not present any more in the Raman spectrum above 13.6 GPa nor to first-order Raman modes of the scheelite phase. Their origin is not known at present but it can be speculated that they could be other strain-activated infrared modes not previously observed. In any case, we have given a tentative explanation for many of the modes appearing in the Raman spectrum of the fergusonite phase of bulk PbMoO_4 , and we think that a similar explanation could give account for the extra Raman modes observed in BaMoO_4 between 5.8 and 9.0 GPa.^{14,15}

Right panel of Fig. 2 shows the pressure dependence of the experimental (empty symbols) and theoretical (lines) Raman mode frequencies of bulk fergusonite- PbMoO_4 from 10 to 20 GPa. Raman modes which do not correspond to first-order modes of the fergusonite phase are marked with small solid symbols: IR-active or second-order modes of scheelite phase (small squares), IR-active or second-order modes of the fergusonite phase (small circles), and first-order modes of the scheelite phase (big solid symbols as those below 10 GPa). Table II summarizes the experimental and theoretical frequencies and pressure coefficients of all the Raman modes in the fergusonite phase of bulk PbMoO_4 at 13.6 GPa. No comparison can be made of our pressure coefficients for the fergusonite phase of wulfenite with other works in the literature since the pressure coefficients of the Raman-active modes of the fergusonite phase were not previously reported.¹⁹

We have tried to assign the symmetries of the different Raman modes of the fergusonite phase with the help of lattice dynamics *ab initio* calculations. Based on our calculations, the assignments of the four stretching modes of the fergusonite phase are clear despite the difference between the experimental and theoretical frequencies and pressure coefficients for the mode of highest frequency, the A_g^8 mode. It is noteworthy

TABLE II. *Ab initio* calculated (Th.) frequencies and pressure coefficients of the Raman modes in bulk fergusonite-type PbMoO₄ at 13.6 GPa. Experimental data of bulk (at 13.6 GPa) and nanocrystalline (Nano.) material (at 14.9 GPa) are reported for comparison.

Peak/mode	Th.		Bulk		Nano.	
	ω (13.6) (cm ⁻¹)	d ω /dP (cm ⁻¹ /GPa)	ω (13.6) (cm ⁻¹)	d ω /dP (cm ⁻¹ /GPa)	ω (14.9) (cm ⁻¹)	d ω /dP (cm ⁻¹ /GPa)
B _g ¹	79.8 (5)	0.37 (3)	72 (3)	0.2 (2)	78 (2)	-0.6 (1)
B _g ²	90.8 (5)	1.50 (3)	94 (3)	2.4 (2)	91 (2)	0.5 (1)
A _g ¹	95 (1)	1.35 (6)	64 (1) ^a	0.2 (1)	64 (1) ^a	0.3 (1)
A _g ²	178 (6)	5.2 (4)	171 (2)	1.7 (1)	159 (3)	1.5 (2)
B _g ³	182 (4)	2.2 (2)	185 (2)	2.3 (1)	204 (5)	2.0 (6)
B _g ⁴	219 (4)	4.2 (2)	231 (3)	1.6 (2)	222 (5)	1.6 (3)
A _g ³	222 (3)	2.0 (3)	251 (2)	0.9 (1)		
B _g ⁵	279 (2)	5.3 (1)	297 (2)	2.7 (1)	278 (7)	3.7 (5)
A _g ⁴	313 (1)	1.94 (4)	325 (2)	1.6 (2)	319 (4)	0.4 (2)
B _g ⁶	345 (2)	2.0 (1)	356 (3)	1.1 (2)	351 (7)	2.1 (4)
A _g ⁵	375 (3)	3.1 (1)	377 (2)	0.9 (1)	389 (9)	3.7 (6)
B _g ⁷	377 (2)	0.9 (1)	402 (2)	2.0 (1)	389 (9)	3.7 (6)
B _g ⁸	433 (3)	4.9 (2)	431 (5)	3.2 (3)	434 (13)	5.5 (7)
A _g ⁶	465 (4)	4.7 (2)	462 (4)	3.5 (2)	466 (12)	6.5 (7)
B _g ⁹	675 (4)	1.1 (2)	699 (4)	0.8 (3)	699 (10)	-0.3 (6)
A _g ⁷	688 (4)	-1.2 (3)	710 (3)	-0.2 (2)	699 (10)	-0.3 (6)
B _g ¹⁰	779 (2)	1.8 (1)	796 (3)	3.7 (2)	777 (4)	3.3 (3)
A _g ⁸	827 (2)	-0.08 (14)	893 (2)	1.5 (1)	859 (10)	-0.3 (5)

^aThis mode has been assigned to the A_g¹ mode despite it is theoretically predicted at much higher frequency.

that our calculations suggest that two of the four high-frequency Raman-active modes of the fergusonite structure should have negative pressure coefficients. In this respect, one of the predicted negative pressure coefficients, that of the A_g⁸ mode, is beyond the uncertainty. In this respect, we have observed the soft-mode behavior of the A_g⁷ mode, despite with a pressure coefficient that differs by 1 cm⁻¹/GPa, but the soft mode behavior of the A_g⁸ is not so clear. In any case, the soft mode or almost pressure-independent behavior of the two A_g stretching modes is a rather curious feature that indicates that MoO₄ tetrahedra in fergusonite-PbMoO₄ are unstable against deformation and suggest that MoO₄ tetrahedra could be deformed in a continuous way into MoO₆ octahedra as occurs in tungstates.^{7,9}

The assignment of the symmetry of the bending modes is rather straightforward but that of the external modes below 150 cm⁻¹ is a little bit more difficult for two reasons: (i) because of the closeness of several modes that are not first-order modes of the fergusonite phase, as already commented, and (ii) because there is a certain discrepancy between the experimental and theoretical frequencies of the lowest-frequency modes. In particular, our calculations predict that the mode with lowest frequency in the fergusonite phase is not the A_g¹ mode but the B_g¹ mode. We have measured that the lowest-frequency mode of the scheelite phase, the soft T(B_g²), is around 63 cm⁻¹ at 10 GPa near the phase transition pressure. This frequency is coincident with the frequency of the lowest-frequency mode observed in the fergusonite phase that according to theoretical calculations it should correspond to the B_g¹ mode. This is somewhat surprising since the second-order scheelite-to-fergusonite phase transition occurring in bulk PbMoO₄ with no volume change^{22,23} should occur via transformation of the soft T(B_g²) mode into the A_g¹

mode with positive pressure coefficient.²⁸ We have indeed observed that the lowest-frequency mode of the fergusonite phase coincides in frequency with the T(B_g²) mode of the scheelite phase at the phase transition pressure and that the new mode exhibits a positive pressure coefficient. These features have led us to assign this mode to the A_g¹ mode despite that theoretically it has been predicted to be at a higher frequency (see Table II). Unfortunately, we cannot comment more on this fact since previous works of molybdates under pressure, in which the transformation of the soft mode of the scheelite phase into the lowest-frequency mode of the fergusonite phase with positive pressure coefficient was observed, do not provide information regarding the symmetry of the lowest-frequency mode of the fergusonite phase.^{11,12,14,15}

Figure 7 shows Raman spectra of nanocrystalline PbMoO₄ from 13.4 GPa till 20 GPa split into two frequency regions. In Fig. 7 it is also shown the Raman spectrum taken at 1 atm after releasing pressure for nanocrystalline PbMoO₄. This spectrum can be attributed to the scheelite phase showing the reversibility of the scheelite to fergusonite phase transition in nanocrystalline PbMoO₄ like in bulk PbMoO₄. Similarly to the case of bulk PbMoO₄, the Raman spectrum at 13.4 GPa shows the presence of new Raman modes in coexistence with Raman modes of the scheelite phase. However, the spectrum at 14.9 GPa shows only Raman modes of the high-pressure phase evidencing that the phase transition is completed at this pressure, which compares with the value of 13.6 GPa for bulk wulfenite. Therefore, our experiments clearly demonstrate that the phase transition is delayed more than 1 GPa in the nanocrystal in comparison to the bulk. This effect is likely caused by the increase of the unit-cell volume associated to reduction of the particle size.³⁴ Our results contrast with recent high-pressure XRD measurements of nanocrystalline

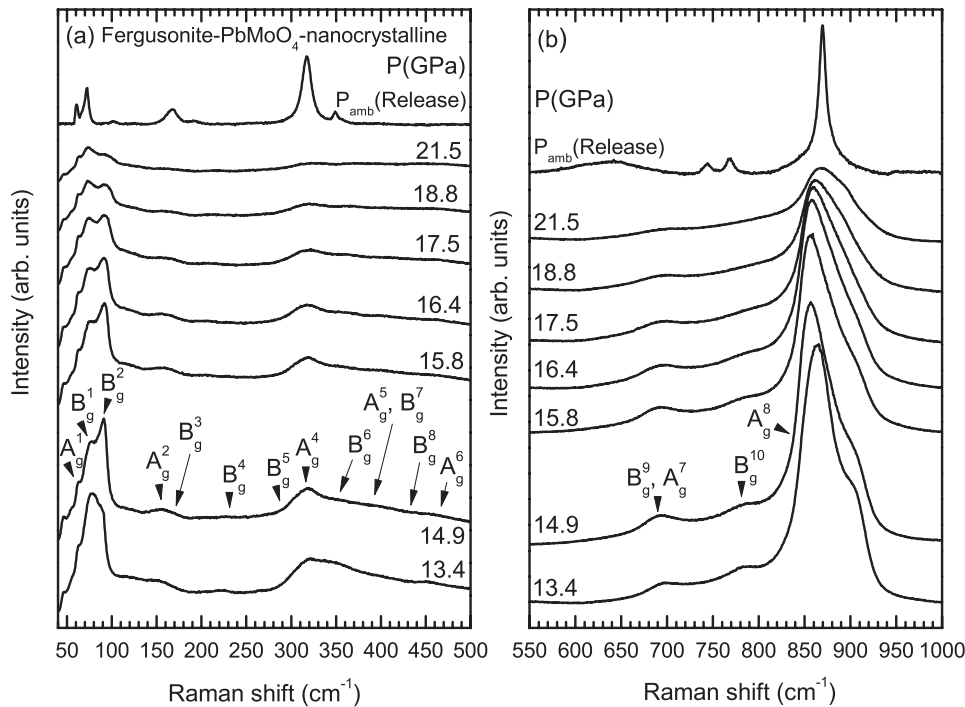


FIG. 7. Room-temperature Raman spectra of the fergusonite phase of nanocrystalline PbMoO_4 at different pressures between 13.4 and 22.0 GPa: (a) low-frequency region and (b) high-frequency region. The assignment of first-order modes of the fergusonite phase is shown in the Raman spectrum at 14.9 GPa. The Raman spectrum at 1 atm after releasing pressure is also shown.

PbMoO_4 that did not show evidence of the scheelite to fergusonite structure transition at least till 16 GPa.²³ We can explain the absence of the phase transition in XRD if we consider several facts: (i) It is usually accepted that the Raman measurements provide a little bit smaller phase transition pressures than XRD measurements;^{7,9} (ii) the scheelite-to-fergusonite phase transition in tungstates and molybdates is a second-order ferroelastic phase transition with no volume change at the phase transition,²⁸ so the fergusonite structure is observed mainly as a broadening of the XRD peaks of the scheelite phase; and (iii) XRD peaks of nanocrystalline PbMoO_4 are already broadened with respect to bulk wulfenite. On the basis of these three considerations, it is clear that it must be difficult to distinguish when nanocrystalline wulfenite XRD peaks get broadened due to the phase transition to the fergusonite phase. Fortunately, Raman scattering measurements are very helpful in distinguishing the subtle changes between both structures since Raman scattering is a more local probe of the structure than XRD measurements and because different Raman modes appear clearly in both scheelite and fergusonite phases.^{7,9}

It is noteworthy that the Raman spectra of the high-pressure phase of nanocrystalline PbMoO_4 is characterized by a gap between 500 and 650 cm^{-1} without first-order Raman bands in good agreement with our expectations for the fergusonite structure. In general, the Raman spectra of the high-pressure phase of nanocrystalline PbMoO_4 exhibit less but broader Raman peaks than those of the high-pressure phase of bulk PbMoO_4 . This means that several modes which are very close in frequency, like the A_g^5 and B_g^7 modes and A_g^7 and B_g^9 modes, have not been resolved. A similar case occurs for the A_g^3 mode, which is very close in frequency to the B_g^4 mode, and has not been observed. Curiously, the four stretching Raman modes of the fergusonite phase are clearly identified as in the case of bulk wulfenite, and no extra Raman modes likely due to IR-activated modes or second-order

modes are observed in the nanocrystalline sample with the exception of a strong shoulder around 900 cm^{-1} ; i.e., above the strong A_g^8 mode of the fergusonite phase. This mode is observed till 21.3 GPa and is already observed in bulk PbMoO_4 and PbWO_4 .⁷ Additionally, a weak feature appears in the Raman spectrum of bulk fergusonite- PbMoO_4 around 930 cm^{-1} [see red arrow in Fig. 6(b)]. We think that both features above the A_g^8 mode of the fergusonite phase can be attributed to second-order modes of the fergusonite phase, and perhaps the stronger intensity of the second-order mode in nanocrystalline fergusonite- PbMoO_4 than in bulk could be attributed to the defect-activation mechanism in the nanocrystalline sample.

Right panel of Fig. 4 shows the pressure dependence of the experimental (open symbols) Raman mode frequencies of nanocrystalline PbMoO_4 from 13.4 to 22 GPa. The theoretical (lines) Raman mode frequencies of bulk PbMoO_4 from 13.4 to 22 GPa have been also shown for comparison. Raman modes which do not correspond to first-order modes of the fergusonite phase are marked with small solid symbols. Table II summarizes the experimental frequencies and pressure coefficients of all the first-order Raman modes of the fergusonite phase in nanocrystalline PbMoO_4 at 14.9 GPa which can be compared to the experimental and theoretical data of bulk wulfenite in the fergusonite phase. As observed in Table II, the frequencies and pressure coefficients of the stretching Raman modes of the fergusonite phase in nanocrystalline wulfenite are rather similar to those of bulk wulfenite with the exception of the already commented A_g^8 mode that displays a slightly soft mode behavior in nanocrystalline PbMoO_4 not clearly observed in bulk material.

V. CONCLUSION

We have performed high-pressure Raman scattering measurements in PbMoO_4 for both bulk and nanocrystalline

powders up to 22 GPa. Our Raman scattering measurements evidence the reversible second-order phase transition from the scheelite structure to the M-fergusonite structure in both bulk and nanocrystalline powders above 10.8 and 13.4 GPa, respectively, in rather good agreement with previous XRD measurements. Our experiments clearly state that the phase transition is delayed more than 1 GPa in the nanocrystal in comparison to the bulk. The pressure dependence of almost all the Raman active modes in both scheelite and fergusonite phases for both bulk and nanocrystalline samples were measured. These results have been compared with theoretical results obtained from lattice dynamics *ab initio* calculations, which have helped us in the assignment of the symmetry of the modes observed in both scheelite and fergusonite phases because, in general, there is a rather good agreement between experiments and calculations.

ACKNOWLEDGMENTS

Financial support from the Spanish ConsoliderIngenio 2010 Program (Project No. CDS2007-00045) is acknowledged. The work was also supported by Spanish MICINN under Projects MAT2010-21270-C04-01/03/04 and from Vicerrectorado de Investigación de la Universitat Politècnica de València under Projects UPV2011-0914PAID-05-11 and UPV2011-0914 PAID-05-11. Supercomputer time has been provided by the Red Española de Supercomputación (RES) and the MALTA cluster.

- ¹C. Lugli, L. Medici, and D. Saccardo, *Neues Jahrbuch fuer Mineralogie - Monatshefte* **6**, 281 (1999).
- ²D. A. Pinnow, L. G. Van Uitert, A. W. Warner, and W. A. Bonner, *Appl. Phys. Lett.* **15**, 83 (1969).
- ³G. A. Coquin, D. A. Pinow, and A. W. Warner, *J. Appl. Phys.* **42**, 2162 (1971).
- ⁴M. Minowa, K. Itakura, S. Moriyama, and W. Otani, *Nucl. Methods Phys. Res. A* **320**, 500 (1992).
- ⁵D. B. Hernández-Uresti, A. Martínez-de la Cruz, and L. M. Torres-Martínez, *Res. Chem. Intermed.* **38**, 817 (2012).
- ⁶D. Errandonea and F. J. Manjón, *Prog. Mater. Sci.* **53**, 711 (2008).
- ⁷F. J. Manjón, D. Errandonea, N. Garro, J. Pellicer-Porres, J. López-Solano, P. Rodríguez-Hernández, S. Radescu, A. Mujica, and A. Muñoz, *Phys. Rev. B* **74**, 144112 (2006).

- ⁸D. Errandonea, J. Pellicer-Porres, F. J. Manjón, A. Segura, Ch. Ferrer-Roca, R. S. Kumar, O. Tschauner, J. López-Solano, P. Rodríguez-Hernández, S. Radescu, A. Mujica, A. Muñoz, and G. Aquilanti, *Phys. Rev. B* **73**, 224103 (2006).
- ⁹F. J. Manjón, D. Errandonea, N. Garro, J. Pellicer-Porres, P. Rodríguez-Hernández, S. Radescu, J. López-Solano, A. Mujica, and A. Muñoz, *Phys. Rev. B* **74**, 144111 (2006).
- ¹⁰D. Errandonea, J. Pellicer-Porres, F. J. Manjón, A. Segura, Ch. Ferrer-Roca, R. S. Kumar, O. Tschauner, P. Rodríguez-Hernández, J. López-Solano, S. Radescu, A. Mujica, A. Muñoz, and G. Aquilanti, *Phys. Rev. B* **72**, 174106 (2005).
- ¹¹D. Christofilos, G. A. Kourouklis, and S. Ves, *J. Phys. Chem. Solids* **56**, 1125 (1995).
- ¹²A. Jayaraman, S. Y. Wang, S. R. Shieh, S. K. Sharma, and L. C. Ming, *J. Raman Spectrosc.* **26**, 451 (1995).
- ¹³W. A. Chrichton and A. Grzechnik, *Z. Kristallogr.* **219**, 337 (2004).
- ¹⁴D. Christofilos, J. Arvanitidis, E. Kampasakali, K. Papagelis, S. Ves, and G. A. Kourouklis, *Phys. Status Solidi B* **241**, 3155 (2004).
- ¹⁵V. Panchal, N. Garg, and S. M. Sharma, *J. Phys.: Condens. Matter* **18**, 3917 (2006).
- ¹⁶D. Errandonea, R. S. Kumar, X. H. Ma, and C. Y. Tu, *J. Solid State Chem.* **181**, 355 (2008).
- ¹⁷D. Errandonea, D. Santamaria-Perez, S. N. Achary, A. K. Tyagi, P. Gall, and P. Gougeon, *J. Appl. Phys.* **109**, 043510 (2011).
- ¹⁸B. N. Ganguly and M. Nicol, *Phys. Status Solidi B* **79**, 617 (1977).
- ¹⁹R. M. Hazen, L. W. Finger, and J. W. E. Mariathasan, *J. Phys. Chem. Solids* **46**, 253 (1985).
- ²⁰A. Jayaraman, B. Batlogg, and L. G. Van Uitert, *Phys. Rev. B* **31**, 5423 (1985).
- ²¹C. Yu, Q. Yu, C. Gao, B. Liu, A. Hao, C. He, X. Huang, D. Zhang, X. Cui, D. Li, H. Liu, Y. Ma, and G. Zou, *J. Phys.: Condens. Matter* **19**, 425215 (2007); C. L. Yu, *et al.*, *Chin. Phys. Lett.* **24**, 2204 (2007).
- ²²Y. X. Liu, *et al.*, *Chin. Phys. C* **33**, 1023 (2009).
- ²³D. Errandonea, D. Santamaría-Pérez, V. Grover, S. N. Achary, and A. K. Tyagi, *J. Appl. Phys.* **108**, 073518 (2010).
- ²⁴K. Syassen, *High Press. Res.* **28**, 75 (2008).
- ²⁵G. Kresse *et al.*, Computer code VASP. See <http://cms.mpi.univie.ac.at/vasp> for more information.
- ²⁶G. Kresse and D. Joubert, *Phys. Rev. B* **59**, 1758 (1999).
- ²⁷A. Mujica, A. Rubio, A. Muñoz, and R. J. Needs, *Rev. Mod. Phys.* **75**, 863 (2003).
- ²⁸D. Errandonea and F. J. Manjón, *Mater. Res. Bull.* **44**, 807 (2009).
- ²⁹A. K. Arora, M. Rajalakshmi, T. R. Ravindran, and V. Sivasubramanian, *J. Raman Spectrosc.* **38**, 604 (2007).
- ³⁰M. Cardona, *High Press. Res.* **24**, 17 (2004).
- ³¹M. Cardona, *Phys. Status Solidi B* **241**, 3128 (2004).
- ³²S. D. Ross, *Inorganic Infrared and Raman Spectra* (McGraw-Hill, Maidenhead, 1972), p. 414.
- ³³J. T. Klopogge and R. L. Frost, *N. Jb. Miner. Mh.* **1**, 193 (1999).
- ³⁴F. J. Manjón, D. Errandonea, J. López-Solano, P. Rodríguez-Hernández, and A. Muñoz, *J. Appl. Phys.* **105**, 094321 (2009).